DOI: 10.1002/ejic.200800421

Chiral Diphosphite-Modified Rhodium(0) Nanoparticles: Catalyst Reservoir for Styrene Hydroformylation

M. Rosa Axet,*[a] Sergio Castillón,[a] Carmen Claver,*[a] Karine Philippot,*[b] Pierre Lecante,[c] and Bruno Chaudret[b]

Keywords: Rhodium / Nanoparticles / Catalysis / Enantioselectivity / Hydroformylation

The organometallic synthesis of rhodium nanoparticles stabilized with diphosphite ligands is described. These nanoparticles were investigated as catalysts in the styrene hydroformylation reaction, and their activity and selectivity were compared with those of similar molecular complexes. NMR spectroscopic studies performed during the course of the catalytic reaction showed that the synthesized nanoparticles are not stable and produce molecular species.

Introduction

The use of metal colloids as catalysts has been attracting growing interest in the past years.[1] Several catalytic reactions have been investigated but hydrogenation is the most studied process. Because it is well known that hydrogenation takes place on metal surfaces, various metal nanoparticles systems have been used in this reaction.[1] More recently, metal nanoparticles have also been used as catalyst for other reactions, such as C–C coupling, where it is more difficult to know if catalysis takes place on the metal surface.[1e,2] The question of the nature of catalysis, namely homogeneous or heterogeneous, is still open, as these processes require different analytical techniques that are difficult to combine for the study of metal nanoparticles.[3] Some authors dealt with this problem by using different approaches, such as by studying reaction kinetics[3b–3d] or by investigating the nature of the intermediate surface species at the surface of the nanoparticles.[4] For example, some of us have recently used various NMR spectroscopic methods to study the reactivity of small molecules towards ruthenium nanoparticle surfaces.[4,5]

The synthesis of metal nanoparticles through hydrogenation of organometallic precursors in the presence of organic ligands has been developed.[6] This method allows metal nanoparticles of various metals (Ru, Pd, Pt or Rh) to be obtained with clean surfaces, and they may be used as catalysts in several chemical reactions such as hydrogenation or C–C coupling.[7] By using this method, an interesting behaviour was observed for palladium nanoparticles stabilized by chiral diphosphite ligands when they are used as catalysts for enantioselective allylic alkylation reactions.[2h,2i] More precisely, it was shown that such palladium nanoparticles display different catalytic reactivities depending on their robustness, which is related to the ligand nature. Although some of them are able to induce high activity and enantioselectivity together with a high degree of kinetic resolution, which is not observed with the related molecular catalytic system, other nanoparticles are less stable and lead to metal leaching and to molecular species activities. On the basis of these previous results, diphosphite chiral ligands were used as stabilizers in the synthesis of rhodium nanoparticles to investigate the influence of the metal precursor and the diphosphite ligand on their catalytic properties.

Rhodium nanoparticles are commonly used as catalysts in hydrogenation reactions,[1] but only a few examples were reported for hydroformylation reactions.[8] Nevertheless, in most cases, the role of the metal nanoparticles in the catalysis is not clear. Some results point out that the nature of the catalyst is heterogeneous,[8d] whereas other studies show that the active species are probably rhodium complexes.[8c,8e] In order to try to shed some light on the behaviour of rhodium nanoparticles in the hydroformylation process, we describe here the synthesis of new chiral diphosphite ligand stabilized rhodium nanoparticles and investigations on their use as catalysts in the hydroformylation of styrene.

[a] Departament de Química Física i Inorgànica, Departament de Química Analítica i Química Orgànica, Universitat Rovira i Virgili,
Marcel.li Domingo s/n, 43007 Tarragona, Spain
Fax: +34-977-559563
E-mail: carmen.claver@urv.cat
[b] Laboratoire de Chimie de Coordination du CNRS, UPR 8241, 205 route de Narbonne, 31077 Toulouse Cedex 04, France
Fax: +33-5-6155303
E-mail: karine.philippot@lcc-toulouse.fr
[c] Centre d'Elaboration des Matériaux et d'Etudes Structurales du CNRS,
29 rue Jeanne Marvig, B. P. 94347, 31055 Toulouse Cedex 04, France

Catalytic tests together with poison tests and high-pressure (HP) NMR spectroscopic studies allowed us to learn the nature of the active species.

Results and Discussion

Synthesis and Characterization of Rhodium Nanoparticles

Rhodium nanoparticles were obtained by decomposition of two different rhodium precursors, $[Rh(\eta^3\text{-}C_3H_5)_3]$[9] and $[Rh(\mu\text{-}OMe)(cod)]_2$,[10] which were synthesised by following previously described methods. As a standard procedure, the decomposition of each rhodium organometallic precursor under an H_2 atmosphere (3 bar) was carried out in thf inside a Fischer–Porter bottle at room temperature and in the presence of the chosen ligand (**1**[11] or **2**;[12] Rh**/L**, 1:0.2; Scheme 1).[6] The decomposition of both rhodium precursors took place in a similar way. The initial pale-yellow solutions became black in a few minutes after dihydrogen introduction, confirming decomposition of the rhodium complexes. The rhodium nanoparticles were isolated as black powders after pentane precipitation and washings affording four samples in the presence of ligands **1** and **2**, respectively, namely, Rh**1** and Rh**2** from $[Rh(\eta^3\text{-}C_3H_5)_3]$ and Rh**3** and Rh**4** from $[Rh(\mu\text{-}OMe)(cod)]_2$.

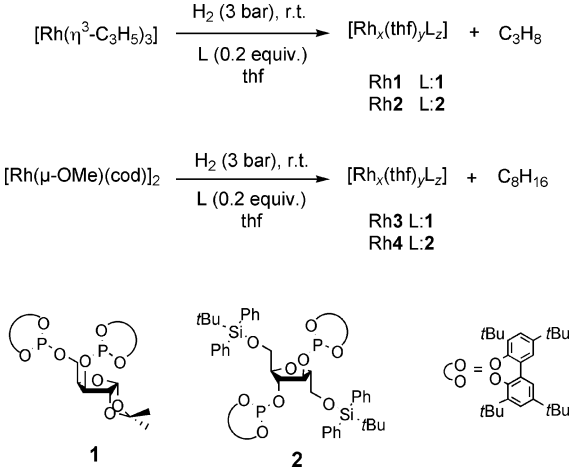

Scheme 1. Synthesis of rhodium nanoparticles from $[Rh(\eta^3\text{-}C_3H_5)_3]$ and $[Rh(\mu\text{-}OMe)(cod)]_2$ in the presence of chiral diphosphite ligands **1** and **2**.

The rhodium nanoparticles were characterized by transmission electron microscopy (TEM), wide-angles X-ray scattering (WAXS) and elemental analysis. Figure 1 presents TEM micrographs and size histograms of samples Rh**1** and Rh**2**. In both cases the nanoparticles are similar, with a small size, a spherical shape and a good dispersion on the TEM grid. Some small agglomerates consisting of a few nanoparticles were also observed. Mean diameters of ca. 3 nm and ca. 2 nm were found for the Rh**1** and Rh**2** nanoparticles, respectively.

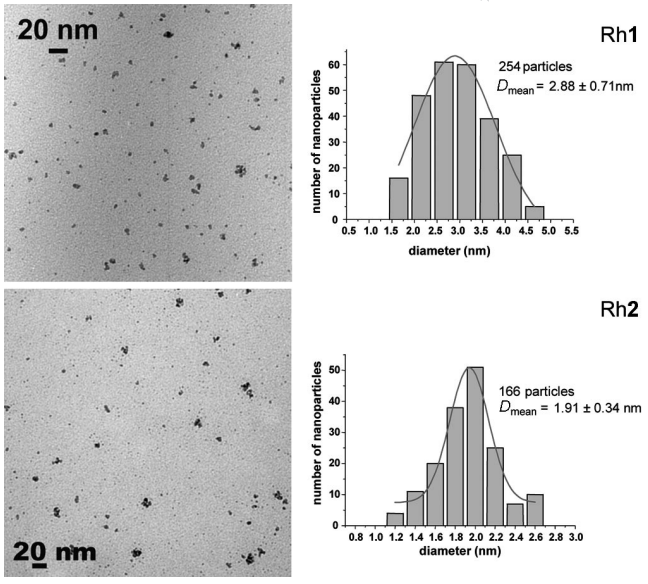

Figure 1. TEM micrographs of Rh**1** and Rh**2** nanoparticles and corresponding size histograms.

The WAXS measurement (Figure 2) revealed in both cases well-crystallized rhodium nanoparticles displaying a fcc (face-centred cubic) structure with a coherence length near 3.5 nm, which is slightly higher than the mean diameter resulting from TEM observations. Nevertheless, Rh**1** contains nanoparticles with a slightly shorter coherence length than Rh**2**, which is in agreement with the size order determined by TEM. In contrast, TEM micrographs of Rh**3** and Rh**4** (Figure 3) revealed large and sponge-like spherical superstructures having a tendency to agglomerate. For Rh**3** these superstructures have a mean diameter of ca. 50 nm and for Rh**4** of ca. 35 nm. Images at higher magnification suggest that these structures are composed of small individual nanoparticles displaying a mean diameter estimated at 4 nm.

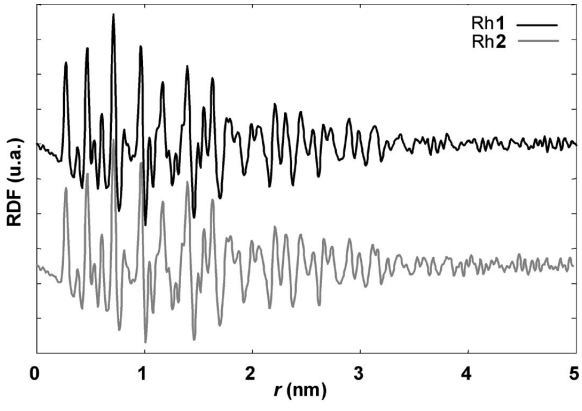

Figure 2. Experimental RDF of rhodium nanoparticles Rh**1** and Rh**2**.

In addition, the WAXS measurement (Figure 4) revealed for both colloids the presence of well-crystallized rhodium domains displaying fcc structure and a coherence length of

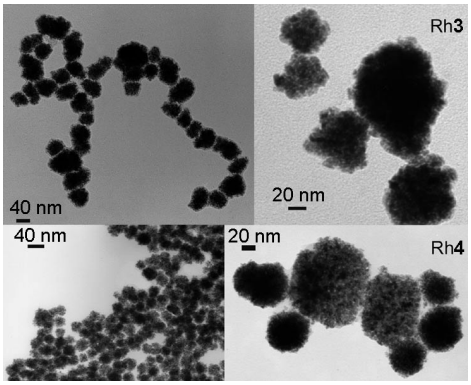

Figure 3. TEM micrographs of Rh**3** (top) and Rh**4** (bottom) nanoparticles.

4 nm, which is in accordance with TEM results. Although TEM and WAXS analysis seem to indicate that these superstructures are agglomerates of small individual nanoparticles, we cannot exclude the possibility that they are large, porous and polycrystalline particles. Similar sponge-like structures have already been observed in the case of rhodium nanoparticles[13] or other metals such as ruthenium,[14] nickel[15] and platinum.[16] From these works, it has been shown that the reaction parameters (metal precursor, method of synthesis, temperature, solvent, etc.) play an important role on the morphology of the nanoparticles. Here we observe a similar phenomenon: the influence of the nature of the rhodium precursor on the morphology of the nanoparticles; $[Rh(\eta^3\text{-}C_3H_5)_3]$ leads to small rhodium nanoparticles, whereas sponge-like structures are obtained with $[Rh(\mu\text{-}OMe)(cod)]_2$. This difference may be explained by taking into account the byproducts resulting from decomposition of each precursor. Indeed, the decomposition of the olefinic precursor $[Rh(\eta^3\text{-}C_3H_5)_3]$ only leads to the production of propane (Scheme 1), which does not interact strongly with the growing metal surface.[6] In contrast, the decomposition of the rhodium $[Rh(\mu\text{-}OMe)(cod)]_2$ complex produces cyclooctane and methanol, which remain in solution (Scheme 1).

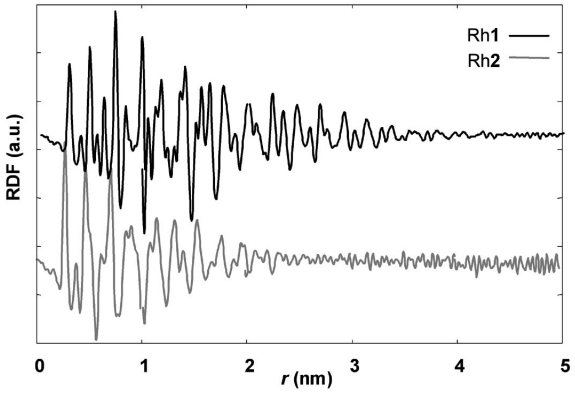

Figure 4. Experimental RDF of rhodium nanoparticles Rh**3** and Rh**4**.

Previous studies reported the role of alcohols in the stabilization of metal nanoparticles through a segregation phase phenomenon.[13,14] In our case, the presence of cyclooctane and methanol in thf may also lead to the formation of droplets segregating from the reaction media in which nanoparticles are confined into agglomerates as previously observed for the synthesis of ruthenium nanoparticles from $[Ru(C_8H_{10})(C_8H_{12})]$ in the presence of alcohols.[14] It is also possible that methanol forms some hydrogen bonds with the phosphorus ligands, which thus leads to agglomeration.

Hydroformylation of Styrene

The use of carbohydrate-derived diphosphites **1** and **2** as ligands in the hydroformylation of vinylarenes catalyzed by rhodium molecular complexes has been previously reported.[11,12,17] As a result of the interesting results provided with these Rh/diphosphite systems we considered testing our diphosphite-stabilized rhodium nanoparticles as catalysts in the hydroformylation reaction. Thus, Rh**3** and Rh**4** nanoparticles were investigated in the rhodium-catalyzed asymmetric hydroformylation of styrene (Scheme 2). The results are given in Tables 1 and 2. The reaction was carried out at 80 or 70 °C, under 20 bar of pressure (pCO/pH$_2$ = 1) with and without the addition of an excess amount of the respective ligand in the catalytic media. The Rh**3** catalytic system showed low conversions (Table 1, Entries 1 and 2), whereas the Rh**4** catalytic system was more active under the same conditions (Table 1, Entries 3 and 4). In both cases the addition of free ligand in the reaction media led to a less active but more regioselective catalytic system (Table 1, Entries 2 and 4 vs. Entries 1 and 3). The enantioselectivity was also affected by the addition of free ligand: from 0 to 40% (*S*) for Rh**3** (Table 1, Entries 1 and 2) and from 13 to 24% (*S*) for Rh**4** (Table 1, Entries 3 and 4).

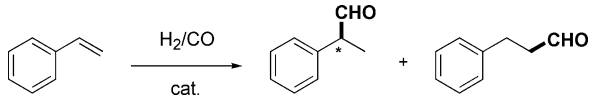

Scheme 2. Hydroformylation reaction of styrene.

Table 1. Styrene hydroformylation with Rh**3** and Rh**4** colloidal catalysts.[a]

Entry	Catalyst	Rh/L/S[b]	t [h]	% Conv.[c]	% Regio.[d]	% *ee*
1	Rh**3**	1:–:200	24	28	57	0
2	Rh**3**	1:0.2:200	24	11	>99	40 (*S*)
3	Rh**4**	1:–:200	24	95	54	13 (*S*)
4	Rh**4**	1:0.2:200	24	80	90	24 (*S*)

[a] Nanoparticle (3 mg), 80 °C, p = 20 bar, pCO/H$_2$ = 1, Rh/S 1:200, styrene (5.8 mmol), toluene (10 mL). [b] Molar ratio between rhodium, excess ligand added to the catalysis and substrate. [c] Percent conversion of styrene determined by GC. [d] Percent of 2-phenylpropanal.

Comparison of the TEM micrographs before and after catalysis (Figure 5) did not show any significant change in the size and shape of the particles. Although this observation could indicate the presence of stable nanoparticles un-

der the catalytic reaction conditions, it was necessary to study more precisely these catalytic systems to know the role of the metal nanoparticles in the catalysis.

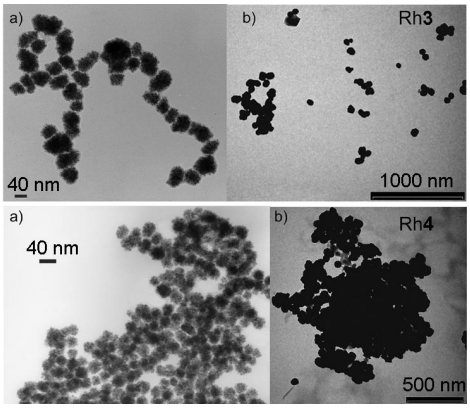

Figure 5. TEM micrographs of Rh**3** (top) and Rh**4** (bottom) nanoparticles: a) before and b) after catalysis.

Firstly, the activities of the two colloidal systems were compared to those of equivalent molecular ones. Table 2 reports the results obtained for the colloidal systems Rh**3** and Rh**4** and for the corresponding molecular systems Mol**3** and Mol**4** prepared in situ. The molecular systems with total conversions after 15 h of reaction (Table 2, Entries 1 and 5) showed higher activity than the colloidal systems (Table 2, Entries 2 and 6). However, the enantioselectivities reached with the colloidal systems were slightly higher than those with the respective molecular systems (Table 2, Entries 1 and 5 vs. Entries 4 and 8). In order to better compare the colloidal and molecular catalytic systems, which display very different reaction rates, a series of complementary experiments was carried out.

Table 2. Styrene hydroformylation with Rh**3** and Rh**4** colloidal systems in comparison with the corresponding molecular systems.[a]

Entry	Catalyst	Rh/L/S[b]	*t* [h]	% Conv.[c]	% Regio.[d]	% *ee*
1	Mol**3**[e]	1:1:200	15	92	95	36 (*S*)
2	Rh**3**	1:0.2:200	15	3	>99	–
3			30	10	>99	–
4			45	35	95	45 (*S*)
5	Mol**4**[f]	1:1:200	15	99	78	20 (*S*)
6	Rh**4**	1:0.2:200	15	31	97	–
7			30	70	95	–
8			45	90	95	31 (*S*)

[a] Nanoparticle (3 mg), 70 °C, p = 40 bar, pCO/H_2 = 1, Rh/S 1:200, styrene (5.8 mmol), toluene (10 mL). [b] Molar ratio between rhodium, excess ligand added to the catalysis and substrate. [c] Percent conversion of styrene determined by GC. [d] Percent 2-phenylpropanal. [e] [Rh] = 9.04×10^{-4} M 70 °C, p = 40 bar, pCO/H_2 = 1, Rh/S 1:200, styrene (1.8 mmol), toluene (10 mL). [f] Substrate/Rh = 200, styrene (2.7 mmol), [Rh(acac)(CO)$_2$] (0.0135 mmol), 60 °C, p = 20 bar, pCO/H_2 = 1, toluene (15 mL).

The catalyst concentration of the homogeneous molecular system Mol**3** was decreased, so that the reaction rates were comparable to those of the colloidal ones. The results are summarized in Table 3. As expected, a decrease in the catalyst concentration gave rise to a decrease in the conversion. However, with dilutions higher than 1:1:2000 (Table 3, Entries 3, 7 and 12) no enantioselectivity was observed. This may be due to the formation of [$RhH(CO)_4$], which is a highly active achiral hydroformylation catalyst.[18] It is known that the formation of this species is favoured at small concentrations of rhodium with respect to the CO quantity in the medium, which displaces the coordinated ligand. To circumvent this phenomenon, free ligand was added in the reaction medium at the same concentration as that used in the colloidal systems (Tables 1 and 2). Under these conditions, lower activities (e.g., Table 3, Entry 3 and 5 vs. Entries 7 and 10) but higher enantioselectivities were observed, as expected. However, at higher dilutions than 1:1:20000 (Table 3, Entries 10, 16 and 22) such addition of free ligand was not enough to maintain the presence of rhodium complex with a coordinated diphosphite ligand, as the enantioselectivity was lower than that observed at lower dilutions.

Table 3. Styrene hydroformylation with diluted Mol**3** catalytic system.[a]

Entry	Rh/L/S[b]	*t* [h]	% Conv.[c]	% Regio.[d]	% *ee*
1	1:1:200[e]	15	92	95	36(*S*)
2	1:1.6:200[e,j]	15	89	96	37(*S*)
3	1:1:2000[f]	15	84	87	0
4	1:7:2000[f,j]	15	35	91	–
5		30	86	95	36 (*S*)
6	1:1:20000[g]	15	35	84	–
7		30	91	79	0
8	1:65:20000[g,j]	15	5	>99	–
9		30	16	>99	–
10		45	85	92	19 (*S*)
11	1:1:100000[h]	15	7	>99	–
12		30	59	85	0
13	1:323:100000[h,j]	15	1	>99	–
14		30	7	>99	–
15		45	15	>99	–
16		60	30	>99	29 (*S*)
17	1:1:200000[i]	15	0	–	–
18		30	<1	>99	–
19	1:645:200000[i,j]	15	<1	>99	–
20		30	8	>99	–
21		45	18	>99	–
22		60	31	>99	29 (*S*)

[a] 70 °C, p = 40 bar, pCO/H_2 = 1, styrene (1.8 mmol), toluene (10 mL). [b] Molar ratio between rhodium, excess ligand added in the catalysis and substrate. [c] Percent conversion of styrene determined by GC. [d] Percent 2-phenylpropanal. [e] [Rh] = 9.04×10^{-4} M. [f] [Rh] = 9.04×10^{-5} M. [g] [Rh] = 9.04×10^{-6} M. [h] [Rh] = 1.81×10^{-6} M. [i] [Rh] = 9.04×10^{-7} M. [j] An excess amount (5.8×10^{-3} mmol) of ligand was added.

The results of these experiments suggest the formation of molecular species, as the diluted molecular system 1:1:10000 (Table 3, Entry 16) leads to similar conversions as those obtained with the colloidal Rh**3** system (Table 2, Entry 4). In order to have more information, we carried out a series of poisoning tests (Tables 4 and 5). CS_2 or Hg was added to the molecular and to the colloidal catalytic systems at the beginning of the reaction (Table 4) and after ≈20% conversion (Table 5).

Table 4. Poison added at the beginning of the styrene hydroformylation reaction with Rh**3** and Mol**3** catalysts.[a]

Entry	Catalyst	Rh/L/S/poison[c]	*t* [h]	% Conv.[d]	% Regio.[e]	% *ee*
1	Mol**3**[b]	1:1:200/–	15	92	95	36 (*S*)
2	Mol**3**[b]	1:1:200:4 (CS_2)	15	96	93	15 (*S*)
3	Mol**3**[b]	1:1:200:100 (Hg)	15	96	92	15 (*S*)
4	Rh**3**	1:0.2:200/–	15	3	>99	–
5			30	10	>99	–
6			45	35	95	45 (*S*)
7	Rh**3**	1:0.2:200:4 (CS_2)	15	14	>99	–
8			30	47	96	40 (*S*)
9			45	64	96	36 (*S*)
10	Rh**3**	1:0.2:200:100 (Hg)	15	3	>99	–
11			30	18	95	33 (*S*)
12			45	38	95	30 (*S*)

[a] Nanoparticle (3 mg), 70 °C, p = 40 bar, pCO/H_2 = 1, Rh/S 1:200, styrene (5.8 mmol), toluene (10 mL). [b] [Rh] = 9.04×10^{-4} M, 70 °C, p = 40 bar, pCO/H_2 = 1, Rh/S 1:200, styrene (1.8 mmol), toluene (10 mL). [c] Molar ratio between rhodium, excess ligand added to the catalysis, substrate and poison. [d] Percent conversion of styrene determined by GC. [e] Percent 2-phenylpropanal.

Table 5. Poison added at ≈20% conversion in the styrene hydroformylation reaction with Rh**3** and Mol**3** catalysts.[a]

Entry	Catalyst	Rh/L/S/poison[c]	*t* [h]	% Conv.[d]	% Regio.[e]	% *ee*
1	Mol**3**[b]	1:1:200/–	3	13	>99	46 (*S*)
2			15	>99	>99	34 (*S*)
3	Mol**3**[b]	1:1:200:4 (CS_2)	15	>99	94	34 (*S*)
4	Mol**3**[b]	1:1:200:100 (Hg)	15	>99	96	34 (*S*)
5	Rh**3**	1:0.2:200/–	45	19	>99	43 (*S*)
6	Rh**3**		90	61	98	44 (*S*)
7	Rh**3**	1:0.2:200:4 (CS_2)	90	50	98	43 (*S*)
8	Rh**3**	1:0.2:200:100 (Hg)	90	58	98	41 (*S*)

[a] Nanoparticle (3 mg), 70 °C, p = 40 bar, pCO/H_2 = 1, Rh/S 1:200, styrene (5.8 mmol), toluene (10 mL). [b] [Rh] = 9.04×10^{-4} M, 70 °C, p = 40 bar, pCO/H_2 = 1, Rh/S 1:200, styrene (1.8 mmol), toluene (10 mL). [c] Molar ratio between rhodium, excess ligand added to the catalysis, substrate and poison. [d] Percent conversion of styrene determined by GC. [e] Percent 2-phenylpropanal.

In all cases we did not observe any significant change in the activity or selectivity between the poisoned and unpoisoned systems. Nevertheless, because it is known that rhodium does not amalgamate with Hg^0[3b] and that CS_2 begins to dissociate from the heterogeneous catalyst at temperatures higher than 50 °C,[3b] whereas the catalytic experiments are carried out at 70 °C, the poisoning tests cannot be considered conclusive. For this reason we carried out in situ HP NMR spectroscopic experiments to study the fate of colloidal Rh**3** catalysts under catalytic conditions. Previously, solution ^{31}P NMR spectra of Rh**3** nanoparticles were recorded in [D_8]toluene or in [D_8]thf (where the nanoparticles were more soluble). In both cases we did not observed any signal. Then, a sapphire tube (ø10 mm) was filled under an atmosphere of argon with Rh**3** and 0.2 equiv. of ligand **1** in [D_8]toluene. The tube was pressurized with CO/H_2 mixture (pCO/H_2 = 40 bar, pCO/$p$$H_2$ = 1). After a reaction time of 45 h during which the solution was shaken at 70 °C, the solution was analyzed at room temperature by NMR spectroscopy. In the ^{1}H NMR spectrum a new signal at –10.15 ppm appeared, whereas in the ^{31}P NMR spectrum a new doublet at δ = 161 ppm ($^1J_{Rh,P}$ = 227 Hz; Figure 6) was observed. These signals correspond to the well-known hydridorhodium diphosphite complex [RhH(CO)$_2$(**1**)] previously described,[11,17] and this species is considered as the resting state in the homogeneous hydroformylation reaction.[18]

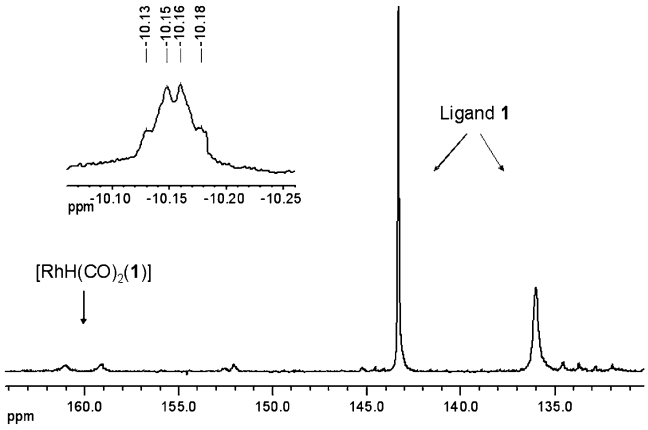

Figure 6. ^{1}H and ^{31}P{^{1}H} NMR spectra of Rh**3** nanoparticles under hydroformylation conditions (T = 70 °C, pCO/H_2 = 40 bar, pCO/$p$$H_2$ = 1) in the presence of ligand **1**.

This indicates that the [RhH(CO)$_2$(**1**)] complex is formed under hydroformylation conditions from rhodium(0) nanoparticles. Therefore, we have evidence that molecular species are formed from rhodium nanoparticles during the reaction, which is probably responsible for the observed catalytic activity even if we cannot exclude the possibility that some activity comes from the rhodium nanoparticles. Such results are in agreement with previous ones, such as the evolution of rhodium(0) nanoparticles into molecular rhodium(I) complexes when used as catalysts in the carbonylation of methanol[19] or in the hydroformylation of 1-alkenes.[8c,8e] These studies report that the nanoparticles are not stable under the reaction conditions and lead to soluble mononuclear rhodium–carbonyl catalytically active species, as we observed in our case by in situ HP NMR spectroscopy. However, such rhodium nanoparticles could be of interest as catalysts in other reactions such as arene hydrogenation where ruthenium nanoparticles stabilized with diphosphite ligands derived from carbohydrates have already shown interesting results.[20]

Conclusions

New rhodium nanoparticles were successfully synthesized in the presence of carbohydrate-derived ligands **1** and **2**. From these results we can say that the shape, size and dispersion of the nanoparticles depend strongly on the metal precursor. We attributed the observed different behaviours to the presence of byproducts in the reaction media that result from decomposition of the precursor, which

leads to a segregation phase phenomenon. Interesting results were also obtained when some of these nanoparticles were tested as catalysts in the rhodium-catalyzed asymmetric hydroformylation of styrene. In particular, different experiments were carried out in order to shed some light on the catalytic species responsible for the activity. Although, the diluted experiments and the poisoning tests were not conclusive, the use of in situ HP NMR under hydroformylation conditions revealed the formation of molecular species that probably are the ones active in the studied reaction. However, we have to highlight that colloidal catalysts reached higher enantioselectivities than the ones obtained with the corresponding diluted molecular system. So, such colloids could be considered as a reservoir for molecular catalysts.

Experimental Section

General Methods: All syntheses were performed by using standard Schlenk and Fisher–Porter bottle techniques under an argon atmosphere, and all other manipulations were performed in an argon-filled glove box. Solvents were purified by standard procedures. Ligands **1**[11] and **2**[12] were prepared by methods described previously. All other reagents were used as commercially available. ^{1}H, $^{13}C\{^{1}H\}$ and $^{31}P\{^{1}H\}$ NMR spectra were recorded with a Varian Gemini 400 MHz spectrometer. Chemical shifts are reported relative to $SiMe_4$ (^{1}H and ^{13}C) as an internal standard or H_3PO_4 (^{31}P) as an external standard. TEM samples were prepared by slow evaporation of a drop of each colloidal solution deposited under an argon atmosphere onto a holey carbon-covered copper grid. The TEM experiments were performed at the "Service Commun de Microscopie Electronique de l'Université Paul Sabatier" (TEMSCAN) in Toulouse with a JEOL 200 CX-T electron microscope operating at 200 kV and a Philips CM12 electron microscope operating at 120 kV with respective resolutions of 4.5 and 5 Å. The TEM analyses of the nanoparticles after catalysis were performed at the "Servei de Recursos Científics" at the University Rovira i Virgili in Tarragona with a Zeiss 10 CA electron microscope at 100 kV with a resolution of 3 Å. The particles size distributions were determined by a manual analysis of enlarged images. At least 150 particles on a given grid were measured in order to obtain a statistical size distribution and a mean diameter. WAXS experiments were performed at the "Centre d'Elaboration des Matériaux et d'Etudes Structurales" (CEMES-CNRS) in Toulouse. All samples were sealed in Lindemann glass capillaries. Measurements of the X-ray intensity scattered by the sample irradiated with graphite-monochromatized Mo-K_α (0.071069 nm) radiation were performed by using a dedicated two-axis diffractometer. Radial distribution functions (RDF) were obtained after Fourier transformation of the reduced intensity functions. Hydroformylation reactions were carried out in a Parr 450-mL multiple reaction vessel autoclave. Gas chromatographic analyses were run on a Hewlett–Packard HP 5890A instrument (split/splitless injector, J&W Scientific, HP-5, 25 m column, internal diameter 0.25 mm, film thickness 0.33 mm, carrier gas: 150 kPa Ar, F.I.D. detector) equipped with a Hewlett–Packard HP3396 series II integrator. Enantiomeric excesses were measured after oxidation of the aldehydes to the corresponding carboxylic acids with a Hewlett–Packard HP 5890A gas chromatograph split/splitless injector, J&W Scientific, Supelco β-DEX 110 (30 m. column, internal diameter 0.25 mm, carrier gas: 100 kPa He, F.I.D. detector).

Synthesis of Rhodium Nanoparticles from the $[Rh(\eta^3\text{-}C_3H_5)_3]$ Precursor: As a standard procedure, $[Rh(\eta^3\text{-}C_3H_5)_3]$ (80 mg, 0.354 mmol) was dissolved under an atmosphere of argon at –110 °C (ethanol/N_2 bath) in tetrahydrofuran (80 mL) containing the chosen ligand (0.2 equiv.) in a closed pressure bottle (75.5 mg of diphosphite **1** for Rh**1** and 107.4 mg of diphosphite **2** for Rh**2**). The Fischer–Porter reactor was then pressurized at room temperature under dihydrogen (3 bar) for 30 min. The initial yellow solution became black after 1 h. Vigorous magnetic stirring and dihydrogen pressure were maintained for 18 h. After that period of time, the hydrogen pressure was eliminated, and a drop of the colloidal solution was deposited under an argon atmosphere on a holey carbon-covered copper grid for electron microscopy analysis. Precipitation with a tetrahydrofuran/pentane mixture at low temperature gave rise to a black precipitate that was washed with pentane (2 × 40 mL) and dried under vacuum. Yield Rh**1**: 23.3 mg (64%); Rh**2**: 39.9 mg (74%). The colloids were characterized by TEM analysis, elemental analysis and WAXS. Elemental analyses of the isolated samples: Rh**1**: C 4.70, H 0.47, P 0.61, Rh 34.23; Rh**2**: C 6.79, H 0.59, P 2.48, Rh 37.74, Si 3.88.

Synthesis of Rhodium Nanoparticles from the $[Rh(\mu\text{-}OMe)(cod)]_2$ Precursor: As a standard procedure $[Rh(\mu\text{-}OMe)(cod)]_2$ (160 mg, 0.330 mmol) was dissolved under an argon atmosphere at –110 °C (ethanol/N_2 bath) in tetrahydrofuran (160 mL) containing the chosen ligand (0.2 equiv.) in a closed pressure bottle (141.2 mg of diphosphite **1** for Rh**3** and 200.6 mg of diphosphite **2** for Rh**4**). The Fischer–Porter reactor was then pressurized at room temperature under dihydrogen (3 bar) for 30 min. The initial yellow solution became black in a few minutes. Vigorous magnetic stirring and hydrogen pressure were maintained for 18 h. After that period of time, the hydrogen pressure was eliminated, and a drop of the colloidal solution was deposited under an argon atmosphere on a holey carbon-covered copper grid for electron microscopy analysis. Precipitation with a tetrahydrofuran/pentane mixture at low temperature gave a black precipitate that was washed with pentane (2 × 40 mL) and dried under vacuum. Yield Rh**3**: 44.5 mg (65%); Rh**4**: 59.0 mg (87%). The colloids were characterized by TEM analysis, elemental analysis and WAXS. Elemental analysis of the isolated samples: Rh**3**: C 2.84, H 0.10, P 0.10, Rh 73.69; Rh**4**: C 4.59, H 0.38, P 0.11, Rh 76.71, Si 5.24.

Hydroformylation Experiments: The catalytic precursors were prepared in a multiple reaction vessel autoclave in a glove box. The experiments with colloidal systems were carried out with the nanoparticles (3 mg), the ligand (5.8×10^{-3} mmol) and styrene (5.8 mmol) in toluene (10 mL). The experiments with molecular systems were carried out with $[Rh(acac)(CO)_2]$ (9×10^{-3} mmol), the ligand (9×10^{-3} mmol) and styrene (1.8 mmol) in toluene (10 mL). After pressurizing with syngas to the desired pressure and heating the autoclave to the chosen temperature, the reaction mixture was stirred for the necessary reaction time. After the given time, the autoclave was cooled to room temperature and depressurized. The reaction mixture was analyzed by gas chromatography. The aldehydes formed through hydroformylation were oxidized into carboxylic acids to determine the enantiomeric excess (*ee*) by gas chromatography.

Poisoning Test Experiments: The catalytic precursors were prepared in a multiple reaction vessel autoclave in a glove box as described previously. After that, CS_2 (4 equiv.) or Hg (100 equiv.) in a ration relative to the introduced rhodium was added at the beginning of the reaction or at ≈20% conversion (3 h for the molecular system and 45 h for the colloidal system). The autoclave was pressurized and heated, and the reaction mixture was stirred as for the other

catalytic tests. After cooling, the reaction mixture was analyzed by gas chromatography. The aldehydes resulting from hydroformylation were oxidized into carboxylic acids to determine the enantiomeric excess (*ee*) by gas chromatography.

In Situ HP NMR Hydroformylation Experiments: A sapphire tube (ø10 mm) was filled under an argon atmosphere with Rh**3** (10 mg) nanoparticles and ligand **1** (19.3×10^{-3} mmol) in [D_8]toluene (2 mL). The HP NMR tube was purged three times with CO and pressurized to the appropriate pressure of CO/H_2 mixture. After a reaction time of 45 h, during which the solution was shaken at 70 °C, the solution was analyzed.

Acknowledgments

We are grateful to the Spanish Ministerio de Educacion y Ciencia (CTQ2007-62288/BQU, Consolider Ingenio 2010, CSD2006-0003) and the Generalitat de Catalunya (2005SGR007777 Distinction for Research Promotion, 2003, C .C.) for financial support. The authors also thank the Departament d'Universitats, Recerca i Societat de la Informació i del Fons Social Europeu for an FPI grant (M. R. A.). K. P. and B. C. thank the TEMSCAN (Service Commun de Microscopie Electronique de l'Université Paul Sabatier) for TEM analysis, Egide (PAI 07165RE) and CNRS (PICS 2428, Picasso 04230PL) for financial support.

[1] a) A. Roucoux, J. Schulz, H. Patin, *Chem. Rev.* **2002**, *102*, 3757–3778; b) A. Roucoux, K. Philippot, "Hydrogenation with Noble Metal Nanoparticles" in *Handbook of Homogeneous Hydrogenations* (Ed.: G. de Vries), Wiley-VCH, Weinheim, **2007**, pp. 217–256; c) M. T. Reetz, R. Breinbauer, K. Wanninger, *Tetrahedron Lett.* **1996**, *37*, 4499–4502; d) M. T. Reetz, E. Westermann, *Angew. Chem. Int. Ed.* **2000**, *39*, 165–168; e) M. Moreno-Mañas, R. Pleixats, S. Villarroya, *Organometallics* **2001**, *20*, 4524–4528; f) C. Rocaboy, J. A. Gladysz, *Org. Lett.* **2002**, *4*, 1993–1996; g) C. C. Cassol, A. P. Umpierre, G. Machado, S. I. Wolke, J. Dupont, *J. Am. Chem. Soc.* **2005**, *127*, 3298–3299; h) D. Astruc, F. Lu, J. Ruiz Aranzaes, *Angew. Chem. Int. Ed.* **2005**, *44*, 7852–7872; i) J. G. de Vries, *Dalton Trans.* **2006**, 421–429; j) J. A. Widegren, R. G. Finke, *J. Mol. Catal. A* **2003**, *191*, 187–207.

[2] a) M. Beller, H. Fischer, K. Kuehlein, C.-P. Reisinger, W. A. Herrmann, *J. Organomet. Chem.* **1996**, *520*, 257–259; b) M. T. Reetz, G. Lohmer, *Chem. Commun.* **1996**, 1921; c) S. Klingelhöfer, W. Heitz, A. Greiner, S. Oestreich, S. Foerster, M. Antonietti, *J. Am. Chem. Soc.* **1997**, *119*, 10116–10120; d) J. Le Bars, U. Specht, J. S. Bradley, D. G. Blackmond, *Langmuir* **1999**, *15*, 7621–7625; e) L. K. Yeung, R. M. Crooks, *Nano Lett.* **2001**, *1*, 14–17; f) Y. Li, E. Boone, M. A. El-Sayed, *Langmuir* **2002**, *18*, 4921–4925; g) R. Narayanan, M. A. El-Sayed, *J. Am. Chem. Soc.* **2003**, *125*, 8340–8347; h) S. Jansat, M. Gomez, K. Philippot, G. Muller, E. Guiu, C. Claver, S. Castillón, B. Chaudret, *J. Am. Chem. Soc.* **2004**, *126*, 1592–1593; i) I. Favier, M. Gómez, G. Muller, M. R. Axet, S. Castillón, C. Claver, S. Jansat, B. Chaudret, K. Philippot, *Adv. Synth. Catal.* **2007**, *349*, 2459–2469.

[3] a) I. W. Davies, L. Matty, D. L. Hughes, P. Reider, *J. Am. Chem. Soc.* **2001**, *123*, 10139–10140; b) J. A. Widegren, R. G. Finke, *J. Mol. Catal. A* **2003**, *198*, 317–341; c) C. M. Hagen, L. Vieille-Petit, G. Laurenczy, G. Süss-Fink, R. G. Finke, *Organometallics* **2005**, *24*, 1819–1831; d) L. Vieille-Petit, G. Süss-Fink, B. Therrien, T. R. Ward, H. Stoeckli-Evans, G. Labat, L. Karmazin-Brelot, A. Neels, T. Bürgi, R. G. Finke, C. M. Hagen, *Organometallics* **2005**, *24*, 6104–6119.

[4] T. Pery, K. Pelzer, G. Buntkowski, K. Philippot, H.-H. Limbach, B. Chaudret, *ChemPhysChem* **2005**, *6*, 605–607.

[5] J. García-Antón, M. R. Axet, S. Jansat, K. Philippot, B. Chaudret, T. Pery, G. Buntkowsky, H.-H. Limbach, *Angew. Chem. Int. Ed.* **2008**, *47*, 2074–2078.

[6] a) K. Philippot, B. Chaudret, *CR. Chim.* **2003**, *6*, 1019–1034; b) B. Chaudret, *C.R. Phys.* **2005**, *6*, 117–131; c) B. Chaudret, in *Topics in Organometallic Chemistry Vol. 16: Surface and Interfacial Organometallic Chemistry and Catalysis*, Springer, Berlin, **2005**, pp. 233–259.

[7] a) A. Roucoux, in *Topics in Organometallic Chemistry Vol. 16: Surface and Interfacial Organometallic Chemistry and Catalysis*, Springer, Berlin, **2005**, pp. 261–279; b) S. Jansat, D. Picurelli, K. Pelzer, K. Philippot, M. Gómez, G. Muller, P. Lecante, B. Chaudret, *New J. Chem.* **2006**, *30*, 115–122.

[8] a) T. W. Smith (Xerox Corporation), US 4252678, **1981**; b) F. Wen, H. Boënnemann, J. Jiang, D. Lu, Y. Wang, Z. Jin, *Appl. Organomet. Chem.* **2005**, *19*, 81–89; c) L. Tuchbreiter, S. Mecking, *Macromol. Chem. Phys.* **2007**, *208*, 1688–1693; d) D. Han, X. Li, H. Zhang, Z. Liu, J. Li, C. Li, *J. Catal.* **2006**, *243*, 318–328; e) A. J. Bruss, M. A. Gelesky, G. Machado, J. Dupont, *J. Mol. Catal. A* **2006**, *252*, 212–218.

[9] a) M. D. Fryzuk, W. E. Piers in *Organometallic Syntheses* (Eds.: R. B. King, J. J. Eisch), Elsevier, Amsterdam, **1986**, vol. 3, p. 128; b) W. A. Herrmann in *Synthetic Methods of Organometallic and Inorganic Chemistry* (Ed.: W. A. Herrmann), Thieme, Stuttgart, **1996**, p. 38.

[10] R. Uson, L. A. Oro, J. A. Cabeza, *Inorg. Synth.* **1985**, *23*, 126.

[11] G. J. H. Buisman, M. E. Martin, E. J. Vos, A. Klootwijk, P. C. J. Kamer, P. W. N. M. van Leeuwen, *Tetrahedron: Asymmetry* **1995**, *6*, 719–738.

[12] M. R. Axet, J. Benet-Buchholz, C. Claver, S. Castillón, *Adv. Synth. Catal.* **2007**, *349*, 1983–1998.

[13] T. D. Ewers, A. K. Sra, B. C. Norris, R. E. Cable, C.-H. Cheng, D. F. Shantz, R. E. Schaak, *Chem. Mater.* **2005**, *17*, 514–520.

[14] a) O. Vidoni, K. Philippot, C. Amiens, B. Chaudret, O. Balmes, J. Malm, J. Bovin, F. Senocq, M. J. Casanove, *Angew. Chem. Int. Ed.* **1999**, *38*, 3736–3738; b) K. Pelzer, O. Vidoni, K. Philippot, B. Chaudret, V. Collière, *Adv. Funct. Mater.* **2003**, *13*, 118–126.

[15] T. Ould Ely, C. Amiens, B. Chaudret, E. Snoeck, M. Verelst, M. Respaud, J.-M. Broto, *Chem. Mater.* **1999**, *11*, 526–529.

[16] a) H. P. Liang, H. M. Zhang, J. S. Hu, Y. G. Guo, L. J. Wan, C. L. Bai, *Angew. Chem. Int. Ed.* **2004**, *43*, 1540–1543; b) G. Schmid, A. Lehnert, J. Malm, J. Bovin, *Angew. Chem. Int. Ed. Engl.* **1991**, *30*, 874–876; c) Y. J. Song, Y. Yang, C. J. Medforth, E. Pereira, A. K. Singh, H. F. Xu, Y. B. Jiang, C. J. Brinker, F. van Swol, J. A. Shelnutt, *J. Am. Chem. Soc.* **2004**, *126*, 635–645.

[17] O. Pámies, G. Net, A. Ruiz, C. Claver, *Tetrahedron: Asymmetry* **2000**, *11*, 1097–1108.

[18] P. W. N. M. van Leeuwen, C. Claver (Eds.), *Rhodium Catalyzed Hydroformylation*, Kluwer Academic, Dordrecht, **2000**, vol. 22..

[19] Q. Wang, H. Liu, M. Han, X. Li, D. Jiang, *J. Mol. Catal. A* **1997**, *l18*, 145.

[20] A. Gual, M. R. Axet, K. Philippot, B. Chaudret, A. Denicourt-Nowicki, A. Roucoux, S. Castillón, C. Claver, *Chem. Commun.*, DOI:10.1039/B802316F.

Received: April 24, 2008
Published Online: July 7, 2008

